The greybody factor for scalar fields in the Schwarzschild spacetime with an $f(R)$ global monopole

Jingyun Man Hongbo Cheng*

Department of Physics, East China University of Science and Technology, Shanghai 200237, China

The Shanghai Key Laboratory of Astrophysics, Shanghai 200234, China

Abstract

The greybody factor of massless scalar fields in the four-dimensional Schwarzschild spacetime involving an $f(R)$ global monopole is derived. We show how the monopole parameter and the deviation from the standard general relativity adjust the greybody factor. We also demonstrate that the effects from the global monopole and $f(R)$ gravity theory are manifest in the energy emission rate and the generalized absorption cross section of the scalar fields.

PACS number(s): 04.70.Bw, 04.70.Dy, 14.80.Hv, 11.80.-m

Keywords: Greybody factor, Black hole, Global monopole, $f(R)$ gravity

*E-mail address: hbcheng@ecust.edu.cn

I. Introduction

In any gravitational theory black holes are the ones of the most relevant objects and have been the focuses while a lot of contributions were paid to them. The black holes could exist at the centre of galaxies [1]. In particle collide the black holes could generate [2, 3]. There are different directions to explore the black holes. The black holes thermodynamics such as their entropy [4-6], thermal radiation [7], phase transition [8-13] were investigated. In addition, a lot of efforts were contributed to the scattering and absorption properties of waves in the spacetime of black hole belonging to the asymptotically flat case [14-20]. The greybody factor defined as the probability for a given wave coming in from infinity to be absorbed by the black hole is directly connected to the absorption cross section and is also discussed [21, 22]. The greybody factors in the four-dimensional Schwarzschild-de Sitter spacetime were computed in the case of minimally coupled scalar field [22-26] or nonminimally coupled ones [27] respectively. In the Schwarzschild-de Sitter spacetime the greybody factor with vanishing angular quantum number in the infrared limit tends to a positive constant for a minimally coupled massless scalar field and goes to zero for the case of a nonminimally coupled ones.

During the process of the vacuum phase transition in the early universe, various kinds of topological defects like domain walls, cosmic strings and monopoles were generated from the breakdown of local or global gauge symmetries [28, 29]. Among these topological defects, a global monopole as a spherical symmetric topological defect occurred in the process of phase transition of a system consisting of a self-coupling triplet of a scalar field whose original global $O(3)$ symmetry is spontaneously broken to $U(1)$. It was found that the metric outside a monopole has a deficit solid angle [30]. Buchdahl put forward a modified gravity theory named as $f(R)$ gravity to explain the accelerated expansion of the universe instead of adding unknown form of dark energy or dark matter [31-34]. The metric around a gravitational source involving a global monopole within the frame of $f(R)$ gravity theory has been studied [35]. The classical motion of a massive test particle around the gravitational object with an $f(R)$ global monopole is discussed [36]. We examine the gravitational lensing for the same object in the strong field limit [37]. We also investigate the thermodynamic quantities of this kind of black hole [38].

The purpose of this paper is to compute the greybody factor for massless scalar fields in the environment of a static and spherically symmetric black hole swallowing an $f(R)$ global monopole. This kind of gravitational sources could contain the global monopole while survive in the universe with accelerated expansion described with the help of $f(R)$ theory. The features of global monopole and $f(R)$ issue may appear simutaneously. We should take into account the role played by the geometrical features of both the global monopole and the modified gravity theory. We can explore the global monopole by means of the greybody factor also corrected by the $f(R)$ gravity theory. It is also significant that we study the greybody factors for massless scalar fields propagating outside this kind of the black hole to understand the $f(R)$ theory in a new direction. We wish to show how the $f(R)$ theory modifies the factors. The influence from the modified gravity on the energy

emission and absorption cross section will also be shown. This could be a new window to observe the effects from global monopole and $f(R)$ theory. At first we introduce the metric outside a black hole containing a global monopole in the context of $f(R)$ gravity theory. A massless scalar field for general coupling ξ, propagating in this spacetime induced by global monopole and the deviation from general relativity except for the source mass is considered. The corresponding greybody factors are also scrutinized. Having derived a complementary low-frequency approximation of the greybody factors with arbitrary coupling ξ, we discuss how the deviation of general relativity relates to the factors analytically and numerically. Further the influence from $f(R)$ issue on the energy emission and the generalized absorption cross section will be presented. Finally the discussions and conclusions are listed.

II. The equation of massless scalar field with coupling ξ around the massive source with an $f(R)$ global monopole

According to Ref. [35], the metric describing the background of the black hole involving an $f(R)$ global monopole is,

$$ds^2 = f(r)dt^2 - \frac{1}{f(r)}dr^2 - r^2(d\theta^2 + \sin^2\theta d\varphi^2) \tag{1}$$

with

$$f(r) = 1 - 8\pi G\eta^2 - \frac{2GM}{r} - \psi_0 r \tag{2}$$

where M is the mass and G is the Newton constant. Here the Lagrangian for the global monopole is $\mathcal{L} = \frac{\infty}{\in}(\partial_\mu\phi^\dashv)(\partial^\mu\phi^\dashv) - \frac{\infty}{\triangle}\lambda(\phi^\dashv\phi^\dashv - \eta^\in)^\in$ with parameters λ, η and the ansatz for the triplet of field configuration $\phi^a = \eta h(r)\frac{x^a}{r}$ while $x^a x^a = r^2$ and $a = 1, 2, 3$. $h(r)$ is a dimensionless function to be determined by its equation of motion [30]. This model has a global $O(3)$ symmetry, which is spontaneously broken to $U(1)$. Here subject to Ref. [35, 36] $f(R)$ is an analytical function of Ricci scalar R and satisfies $\frac{df(R)}{dR} = 1 + \psi_0 r$. Now the correction to the general relativity is limited as $\psi_0 r \ll 1$. The tiny factor ψ_0 reflects the deviation of standard general relativity and then the $f(R)$ gravity model could explain the cosmic acceleration. It should be pointed out that the model parameter η is of the order $10^{16}GeV$ for a typical grand unified theory, which means $8\pi G\eta^2 \approx 10^{-5}$. If we choose $\psi_0 = 0$ excluding the modification from $f(R)$ theory, the metric (2) will recover to be the result by Barriola and Vilenkin [30].

We find that the black hole horizion and the cosmological horizon of metric (2) are located at,

$$r_\pm = \frac{(1 - 8\pi G\eta^2) \pm \sqrt{(1 - 8\pi G\eta^2)^2 - 8\psi_0 GM}}{2\psi_0} \tag{3}$$

which reduce to a black hole with a global monopole who has only one event horizon $r_H = \frac{2GM}{1-8\pi G\eta^2}$. In this metric (2) we study a massless scalar field $\Phi(x^\mu)$ coupled to the gravitational field. The action for this scalar field is [40],

$$S = \frac{1}{2}\int d^4x\sqrt{-g}(\nabla_\mu\Phi\nabla^\mu\Phi + \xi R\Phi^2) \tag{4}$$

where g is the determinant of the spacetime metric and ξ is the coupling between the scalar field and the gravitational fields. Equivalently this massless scalar field satisfies the Klein-Gordon equation,

$$(\nabla_\mu\nabla^\mu + \xi R)\Phi(x) = 0 \tag{5}$$

In order to solve the Eq. (5), we write the solution in the following form [40],

$$\begin{aligned}\Phi(x) &= \Phi(t, r, \theta, \varphi) \\ &= \frac{\psi_{\omega l}(r)}{r} Y_{lm}(\theta, \varphi) e^{-i\omega t}\end{aligned} \tag{6}$$

where ω is the frequency. $Y_{lm}(\theta, \varphi)$ are the scalar spherical harmonics. The radial part of the solution to Eq. (5) obeys the following equation,

$$f\frac{d}{dr}(f\frac{d\psi_{\omega l}}{dr}) - V(r)\psi_{\omega l} + \omega^2\psi_{\omega l} = 0 \tag{7}$$

where

$$V(r) = f[\xi f'' + (4\xi + 1)\frac{f'}{r} + 2\xi\frac{f}{r^2} + \frac{l(l+1) - 2\xi}{r^2}] \tag{8}$$

is the potential and the prime stands for the derivative with respect to r and l is the angular quantum number. The terms with coupling constant in Eq. (7) changes the evolution of a scalar field in the background of a Schwarzschild black hole with a $f(R)$ global monopole.

III. The greybody factor for massless scalar field with coupling ξ around the massive source with an $f(R)$ global monopole

We plan to determine analytically the greybody factors for the radiation of a emitted scalar particle generated by a Schwarzschild black hole with a $f(R)$ global monopole. We follow the procedure of Ref. [27, 39] to investigate the metric. The nonlinear equation (7) is very difficult to obtain the analytic solution directly. We adopt the low-frequency approximation by solving the radial equation in near-region where r is close to the black hole horizon and far-region close to the cosmological horizon and matching two results in the intermediate region. Both the energy emission rate and the absorption cross section are dependent on the ratio of the coefficient $A_{\omega l}^{out}$ and $A_{\omega l}^{in}$ yielded in solutions of the nonlinear equation. The condition that two wave solutions in near and far region can be overlapped in a intermediate region is $\omega \ll 1/MG$, which demands low energy for the emission of a scalar field in black hole spacetime. We define the near-region where $r - r_- \ll \frac{1}{\omega}$, and the far-region as $r - r_- \ll MG$. Then one can match two kinds of wave in the overlapping range $MG \ll r - r_- \ll \frac{1}{\omega}$.

The metric $f(r) = 0$ when the radial coordinate goes to either the inner horizon or the outer horizon, which leads a vanished potential. Near the inner event horizon of the black hole with an $f(R)$ global monopole, for no outgoing flux across the black hole horizon, the solution to Eq. (7) can be written as [27],

$$\psi_{\omega l}(r) \approx A^{tr}_{\omega l} e^{-i\omega r_*} \tag{9}$$

where r_* is the tortoise coordinate defined by $\frac{dr_*}{dr} \equiv \frac{1}{f}$. The solution near the outer event horizon of this kind of black hole can be denoted as,

$$\psi_{\omega l}(r) \approx A^{in}_{\omega l} e^{-i\omega r_*} + A^{out}_{\omega l} e^{i\omega r_*} \tag{10}$$

where $A^{in}_{\omega l}$ and $A^{out}_{\omega l}$ represent the amplitudes of the incoming wave and the outgoing wave respectively. According to the definition, the greybody factors can be written as [27],

$$\gamma_l(\omega) = |\frac{A^{tr}_{\omega l}}{A^{in}_{\omega l}}|^2 = 1 - |\frac{A^{out}_{\omega l}}{A^{in}_{\omega l}}|^2 \tag{11}$$

because of $|A^{in}_{\omega l}|^2 = |A^{tr}_{\omega l}|^2 + |A^{out}_{\omega l}|^2$ from flux conservation. If we estimate the coefficients $A^{in}_{\omega l}$ and $A^{out}_{\omega l}$, the greybody will be confirmed.

A black hole act like a greybody not a perfect blackbody because the spectrum of a particle emitted by a black hole or a blackbody are significantly different in low-frequency while in high-frequency they agree well. Analytically the absorption probability with vanished angular quantum number and no coupling to gravitational field are given by $\frac{4r_+^2 r_-^2}{(r_+^2+r_-^2)^2}$ [39]. However, the nonminimal coupling constant contributes a zero greybody factor with $l = 0$ when $\omega \to 0$ [27]. For these reasons, absorption probability in low-energy, $\omega \ll 1/MG$, contains the information about the structure of spacetime around a black hole.

It is important to research on the amplitudes of the incoming wave and the outgoing wave. Let

$$R_{\omega l}(r) = \frac{\psi_{\omega l}(r)}{r} \tag{12}$$

then rewrite the Eq. (7) as,

$$\frac{d}{dr}(r^2 f \frac{dR_{\omega l}}{dr}) + [-\xi R r^2 + \frac{\omega^2}{f} r^2 - l(l+1)] R_{\omega l} = 0 \tag{13}$$

where the Ricci scalar curvature is

$$R = f'' + \frac{4f'}{r} + \frac{2f}{r^2} - \frac{2}{r^2} \tag{14}$$

We solve the equation of radial parts like Eq. (13) near the event horizons because the amplitudes exist in these regions. When the radial coordinate $r \longrightarrow r_-$, the $f(R)$ gravity term $\psi_0 r$ in metric verges to zero, then Eq. (13) will be approximated to be,

$$y(1-y)\frac{d^2R^n_{\omega l}}{dy^2}+(1-y)\frac{dR^n_{\omega l}}{dy}+[\frac{16\pi\xi G\eta^2-l(l+1)}{1-8\pi G\eta^2}\frac{1}{1-y}+\frac{\omega^2r_-^4}{(2GM)^2}\frac{1-y}{y}]R^n_{\omega l}=0 \tag{15}$$

where

$$y=1-\frac{2GM}{1-8\pi G\eta^2}\frac{1}{r} \tag{16}$$

Here $R_{\omega l}(r)$ near the inner horizon is written as $R^n_{\omega l}(r)$. We choose,

$$R^n_{\omega l}=y^{i\varpi}(1-y)^{L+1}F_{\omega l} \tag{17}$$

$$L(L+1)=\frac{l(l+1)-16\pi\xi G\eta^2}{1-8\pi G\eta^2} \tag{18}$$

$$\varpi=\frac{r_-^2}{2GM}\omega \tag{19}$$

where L can be regarded as modified number which is connected with angular quantum, global monopole parameter and the coupling constant. It reduces to l without global monopole in black hole. Substitute these equations (17), (18), (19) into Eq. (15) to obtain,

$$\begin{aligned}y(1-y)\frac{d^2F_{\omega l}}{dy^2}+\{(2i\varpi+1)-[(2i\varpi+L+1)+(L+1)+1]y\}\frac{dF_{\omega l}}{dy}\\ -(2i\varpi+L+1)(L+1)F_{\omega l}=0\end{aligned} \tag{20}$$

which is the hypergeometric equation [41]. The solution to Eq. (20) is certainly written as hypergeometric functions [41],

$$\begin{aligned}F_{\omega l}=&C_1F(2i\varpi+L+1,L+1,2i\varpi+1,y)\\ &+C_2y^{-2i\varpi}F(L+1,L-2i\varpi+1,1-2i\varpi,y)\end{aligned} \tag{21}$$

According to Eq. (17), the radial parts of the solution is,

$$\begin{aligned}R^n_{\omega l}=&C_1y^{i\varpi}(1-y)^{L+1}F(2i\varpi+L+1,L+1,2i\varpi+1,y)\\ &+C_2y^{-i\varpi}(1-y)^{L+1}F(L+1,L-2i\varpi+1,1-2i\varpi,y)\end{aligned} \tag{22}$$

where $y^{i\varpi}$ term represents an outgoing wave at the black hole horizon and $y^{-i\varpi}$ term implies an incoming wave when $y=0$. According to the boundary condition, only incoming mode exists at near-region , which means $C_1=0$. In the low-frequency limit, the radial part becomes,

$$R^n_{0l} = \lim_{\omega \longrightarrow 0} R^n_{\omega l}$$
$$= C(1-y)^{L+1} F(L+1, L+1, 1, y) \tag{23}$$

where C is a coefficient. According to the Pfaff theorem for the hypergeometric function and the Murphy expressions for the Legendre polynomials [41], the asymptotic form of the radial part is,

$$R^n_{0l} = C(-1)^L P_L(1 - \frac{1-8\pi G\eta^2}{GM} r) \tag{24}$$

In the region near the outer event horizon where $r - r_- \gg MG$, the mass term $2GM/r$ in the metric (2) vanishes, so the radial wave equation is changed as

$$x(1-x)\frac{d^2 R^f_{\omega l}}{dx^2} + (1-3x)\frac{dR^f_{\omega l}}{dx}$$
$$+[6\xi - \frac{l(l+1) - 16\pi\xi G\eta^2}{(1-8\pi G\eta^2)(1-x)} + \frac{\omega^2}{\psi_0^2}\frac{1-x}{x}]R^f_{\omega l} = 0 \tag{25}$$

where

$$x = 1 - \frac{\psi_0 r}{1 - 8\pi G\eta^2} \tag{26}$$

and,

$$R^f_{\omega l} = x^{i\tilde{\omega}}(1-x)^L \tilde{F}_{\omega l} \tag{27}$$

$$\tilde{\omega} = \frac{\omega}{\psi_0} \tag{28}$$

The wave equation is denoted as a hypergeometric equation,

$$x(1-x)\frac{d^2\tilde{F}_{\omega l}}{dx^2} + [(2i\tilde{\omega}+1) - (2i\tilde{\omega} + 2L + 3)x]\frac{d\tilde{F}_{\omega l}}{dx}$$
$$-[2i\tilde{\omega}(L+1) + L(L+2) - 6\xi]\tilde{F}_{\omega l} = 0 \tag{29}$$

The solution to Eq. (29) is [41],

$$\tilde{F}_{\omega l} = D_1 F(\alpha_+, \alpha_-, \gamma, x) + D_2 x^{1-\gamma} F(\alpha_+ - \gamma + 1, \alpha_- - \gamma + 1, 2 - \gamma, x) \tag{30}$$

where

$$\alpha_\pm = (i\tilde{\omega} + L + 1) \pm \sqrt{-\tilde{\omega}^2 - 2i\tilde{\omega} - 2L - 1 + 6\xi} \tag{31}$$

$$\gamma = 2i\tilde{\omega} + 1 \tag{32}$$

The solution near the outer horizon is,

$$R^f_{\omega l} = D_1 x^{i\tilde{\omega}}(1-x)^L F(\alpha_+, \alpha_-, \gamma, x) \\ + D_2 x^{-i\tilde{\omega}}(1-x)^L F(\alpha_+ - \gamma + 1, \alpha_- - \gamma + 1, 2-\gamma, x) \tag{33}$$

When the radial coordinate approaches the larger radius of the metric, then $\lim_{r \longrightarrow r_+} f(r) = 1 - 8\pi G\eta^2 - \psi_0 r$, and we can write the tortoise coordinate as $e^{i\omega r_*} = x^{-i\tilde{\omega}}$, which leading the solution (33) to be

$$R^f_{\omega l} \approx D_1 x^{i\tilde{\omega}} + D_2 x^{-i\tilde{\omega}} \tag{34}$$

At this position we combine Eq. (12) with Eq. (10) to obtain,

$$R^f_{\omega l} \approx \frac{A^{in}_{\omega l}}{r_+} x^{i\tilde{\omega}} + \frac{A^{out}_{\omega l}}{r_+} x^{-i\tilde{\omega}} \tag{35}$$

and then,

$$A^{in}_{\omega l} = r_+ D_1 \tag{36}$$

$$A^{out}_{\omega l} = r_+ D_2 \tag{37}$$

It is clear that the greybody factors can be shown in terms of the coefficients D_1 and D_2 from Eq. (11) [27],

$$\gamma_l(\omega) = 1 - |\frac{D_2}{D_1}|^2 \tag{38}$$

It is reasonable to match the two asymptotic solutions in Eq. (22) and Eq. (33) in the overlapping region of their own districts to relate coefficients D_1 and D_2 with C_1 or C_2 mentioned in Eq. (22) like Ref. [27]. We are also interested in the near-region solution with larger radial coordinate and the far-region solution with smaller r. Using the $y \to 1-y$ transformation law for the hypergeometric function, Eq. (22) is expressed as

$$R^n_{\omega l} = C_2 y^{-i\varpi}(\frac{2GM}{1-8\pi G\eta^2}\frac{1}{r})^{L+1}\frac{\Gamma(1-2i\varpi)\Gamma(-2L-1)}{\Gamma(-2i\varpi-L)\Gamma(-L)} \\ \times F(L+1, L-2i\varpi+1, 2L+2; 1-y) \\ + C_2 y^{-i\varpi}(\frac{2GM}{1-8\pi G\eta^2}\frac{1}{r})^{-L}\frac{\Gamma(1-2i\varpi)\Gamma(2L+1)}{\Gamma(L+1)\Gamma(L-2i\varpi+1)} \\ \times F(-2i\varpi-L, -L, -2L; 1-y) \tag{39}$$

The hypergeometric functions in Eq. (33) are also transformed to give rise to,

$$
\begin{aligned}
R^f_{\omega l} = D_1 x^{i\tilde{\omega}}(\frac{\psi_0 r}{1-8\pi G\eta^2})^L \frac{\Gamma(\gamma)\Gamma(\gamma-\alpha_+-\alpha_-)}{\Gamma(\gamma-\alpha_+)\Gamma(\gamma-\alpha_-)} \\
\times F(\alpha_+,\alpha_-,\alpha_++\alpha_--\gamma+1;1-x) \\
+D_1 x^{i\tilde{\omega}}(\frac{\psi_0 r}{1-8\pi G\eta^2})^{-L-1} \frac{\Gamma(\gamma)\Gamma(\alpha_++\alpha_--\gamma)}{\Gamma(\alpha_+)\Gamma(\alpha_-)} \\
\times F(\gamma-\alpha_+,\gamma-\alpha_-,\gamma-\alpha_+-\alpha_-+1;1-x) \\
+D_2 x^{-i\tilde{\omega}}(\frac{\psi_0 r}{1-8\pi G\eta^2})^L \frac{\Gamma(2-\gamma)\Gamma(\gamma-\alpha_+-\alpha_-)}{\Gamma(1-\alpha_+)\Gamma(1-\alpha_-)} \\
\times F(\alpha_+-\gamma+1,\alpha_--\gamma+1,\alpha_++\alpha_--\gamma+1;1-x) \\
+D_2 x^{-i\tilde{\omega}}(\frac{\psi_0 r}{1-8\pi G\eta^2})^{-L-1} \frac{\Gamma(2-\gamma)\Gamma(\alpha_++\alpha_--\gamma)}{\Gamma(\alpha_+-\gamma+1)\Gamma(\alpha_--\gamma+1)} \\
\times F(1-\alpha_+,1-\alpha_-,\gamma-\alpha_+-\alpha_-+1;1-x)
\end{aligned} \tag{40}
$$

The matching condition is [27],

$$
\lim_{y\longrightarrow 1} R^n_{\omega l} = \lim_{x\longrightarrow 1} R^f_{\omega l} \tag{41}
$$

We substitute Eq. (39) and Eq. (40) into Eq. (41) and compare the coefficients of term r^L and r^{-L-1} respectively to obtain,

$$
\begin{aligned}
D_1(\frac{\psi_0}{1-8\pi G\eta^2})^L \frac{\Gamma(\gamma)\Gamma(\gamma-\alpha_+-\alpha_-)}{\Gamma(\gamma-\alpha_+)\Gamma(\gamma-\alpha_-)} \\
+D_2(\frac{\psi_0}{1-8\pi G\eta^2})^L \frac{\Gamma(2-\gamma)\Gamma(\gamma-\alpha_+-\alpha_-)}{\Gamma(1-\alpha_+)\Gamma(1-\alpha_-)} \\
= C_2(\frac{2GM}{1-8\pi G\eta^2})^{-L} \frac{\Gamma(1-2i\varpi)\Gamma(2L+1)}{\Gamma(L+1)\Gamma(L-2i\varpi+1)}
\end{aligned} \tag{42}
$$

$$
\begin{aligned}
D_1(\frac{\psi_0}{1-8\pi G\eta^2})^{-L-1} \frac{\Gamma(\gamma)\Gamma(\alpha_++\alpha_--\gamma)}{\Gamma(\alpha_+)\Gamma(\alpha_-)} \\
+D_2(\frac{\psi_0}{1-8\pi G\eta^2})^{-L-1} \frac{\Gamma(2-\gamma)\Gamma(\alpha_++\alpha_--\gamma)}{\Gamma(\alpha_+-\gamma+1)\Gamma(\alpha_--\gamma+1)} \\
= C_2(\frac{2GM}{1-8\pi G\eta^2})^{L+1} \frac{\Gamma(1-2i\varpi)\Gamma(-2L-1)}{\Gamma(-2i\varpi-L)\Gamma(-L)}
\end{aligned} \tag{43}
$$

Having solved Eq. (42) and Eq. (43), we arrive at the analytic approximation for greybody factor,

$$
\begin{aligned}
\gamma_l(\omega) = 1 - \\
|[(\frac{2\psi_0 GM}{(1-8\pi G\eta^2)^2})^{2L+1} \frac{\Gamma(2i\tilde{\omega}+1)\Gamma(1-2i\varpi)(\Gamma(-2L-1))^2}{\Gamma(\gamma-\alpha_+)\Gamma(\gamma-\alpha_-)\Gamma(-L-2i\varpi)\Gamma(-L)} \\
-\frac{\Gamma(2i\tilde{\omega}+1)\Gamma(1-2i\varpi)(\Gamma(2L+1))^2}{\Gamma(L-2i\varpi+1)\Gamma(\alpha_+)\Gamma(\alpha_-)\Gamma(L+1)}] \\
\times[\frac{\Gamma(1-2i\varpi)\Gamma(1-2i\tilde{\omega})(\Gamma(2L+1))^2}{\Gamma(L-2i\varpi+1)\Gamma(\alpha_+-\gamma+1)\Gamma(\alpha_--\gamma+1)\Gamma(L+1)} \\
-(\frac{2\psi_0 GM}{(1-8\pi G\eta^2)^2})^{2L+1} \frac{\Gamma(1-2i\tilde{\omega})\Gamma(1-2i\varpi)(\Gamma(-2L-1))^2}{\Gamma(1-\alpha_+)\Gamma(1-\alpha_-)\Gamma(-L-2i\varpi)\Gamma(-L)}]^{-1}|^2
\end{aligned} \tag{44}
$$

The dependence of greybody factor on the frequency due to the model parameter η is plotted in the Figure groups consisting of Fig. 1, Fig. 2 and Fig. 3 with angular quantum number $l = 0, 1, 2$ respectively. When the quantum number vanishes, the greybody factor becomes smaller as the parameter η changes to be small. In the case of nonvanishing angular quantum number, the curves of absorption probability rise while the global monopole parameter decreases. Noticing the magnitude of greybody factor is getting smaller as l increases, we extend the frequency axis to 0.01 to see the behavior of the function. Combined with the energy emission rate in section IV, we find out a significant property that with a large decreasing global monopole parameter the summation of nonvanishing angular quantum number leads a increasing energy emission, however, the parameter η decreases tiny enough so that the first order greybody factor $\gamma_0(\omega)$ dominates over all others.

In order to understand how the deviation of standard general relativity effect the absorption probability, we derive the greybody factor in Schwarzschild spacetime with a global monopole. Fortunately, the Eq. (25) in the region close to the inner horizon and the solution belonging to it are suitable for the this new case with no $f(R)$ gravity involved. Hence, we just need to resolve Eq. (13) to find the asymptotic solution with regarded metric $f(r) = 1 - 8\pi G\eta^2 - \frac{2GM}{r}$. With asymptotic approach and series expansion at $r \to \infty$ to first order for each term, Eq. (13) can be written as [42-44],

$$\frac{d^2 R_{\omega l}^{fM}}{dr^2} + \frac{2}{r}\frac{dR_{\omega l}^{fM}}{dr} + \left(\frac{\omega^2}{(1-8\pi G\eta^2)^2} - \frac{L(L+1)}{r^2}\right) R_{\omega l}^{fM} = 0 \tag{45}$$

This is a Bessel equation of which the solution in asymptotic region is given by

$$R_{\omega l}^{fM} = \frac{1}{\sqrt{r}}\left[B_1 J_{L+\frac{1}{2}}\left(\frac{\omega r}{1-8\pi G\eta^2}\right) + B_2 Y_{L+\frac{1}{2}}\left(\frac{\omega r}{1-8\pi G\eta^2}\right)\right] \tag{46}$$

Taking $r \to 0$, $R_{\omega l}^{fM}$ at intermediate-region with low energy can be expressed as

$$R_{\omega l}^{fM} \approx \frac{B_1 r^L}{\Gamma(L+\frac{3}{2})}\left(\frac{\omega r}{2(1-8\pi G\eta^2)}\right)^{L+\frac{1}{2}} - \frac{B_2\Gamma(L+\frac{1}{2})}{\pi r^{L+1}}\left(\frac{\omega r}{2(1-8\pi G\eta^2)}\right)^{-L-\frac{1}{2}} \tag{47}$$

Compare Eq. (47) with Eq. (39) at $y \to 1$, one may find the ratio of B_1 and B_2

$$\begin{aligned} B &\equiv \frac{B_1}{B_2} \\ &= -\frac{1}{\pi}\left(\frac{(1-8\pi G\eta^2)^2}{GM\omega}\right)^{2L+1}\frac{(L+\frac{1}{2})\Gamma^2(L+\frac{1}{2})\Gamma(2L+1)\Gamma(-L)\Gamma(-L-i\frac{4GM\omega}{(1-8\pi G\eta^2)^2})}{\Gamma(L+1)\Gamma(L+1-i\frac{4GM\omega}{(1-8\pi G\eta^2)^2})\Gamma(-2L-1)} \end{aligned} \tag{48}$$

The absorption probability with low-frequency limit can be approximated as (see [27]),

$$\gamma_l(\omega) \approx \frac{2i(B^* - B)}{|B|^2} \tag{49}$$

where the star index stands conjugation. We plot the dependence of the absorption probability on the $f(R)$ gravity factor ψ_0 in Fig. 4, 5, 6 as the angular quantum number $l = 0, 1, 2$ respectively. The

solid curves in three graphs show the behavior of greybody factor of emission without the effect from gravity correction. For low-frequency ($\omega \ll 1/MG, MG = 1$), the absorption probability curve rises as the deviation from the general relativity ψ_0 increases, which means the more deviation exists, the larger greybody factor of a emitted scalar field coupling to gravitational field can be obtained. The total order of magnitude of greybody factor gets smaller as the angular index increases. This feature conform with the absorption probability $\gamma_l \approx \omega^{2l+2}$ in low-frequency approximation $\omega \ll 1/MG$, which shows the first partial absorption probability is the leadership. It should be pointed out that the greybody factor is an increasing function of frequency no matter how many the angular quantum number is equal to and how great the model parameter or the deviation from general relativity is.

IV. The energy emission rate and the generalized absorption cross section with an $f(R)$ global monopole

Here we discuss the flux spectrum which is the number of massless scalar particles emitted by the gravitational source per unit time and is given by [27, 39],

$$\frac{dN(\omega)}{dt} = \frac{1}{2\pi}\frac{1}{e^{\frac{\omega}{T_H}}-1}\left(\sum_{l=0}^{\infty}(2l+1)\gamma_l(\omega)\right)d\omega \tag{50}$$

leading the differential energy emission rate [27, 39],

$$\begin{aligned}\frac{d^2E(\omega)}{dtd\omega} &= \frac{d^2N(\omega)}{dtd\omega}\omega \\ &= \frac{1}{2\pi}\frac{\omega}{e^{\frac{\omega}{T_H}}-1}\sum_{l=0}^{\infty}(2l+1)\gamma_l(\omega)\end{aligned} \tag{51}$$

where T_H is the Hawking temperature which is $\frac{1}{4\pi}\left(\frac{1-8\pi G\eta^2}{r_-}-2\psi_0\right)$. We show our numerical results for the differential energy emission rate in Fig. 7. One can see as the model parameter η reduces, the maximum of emission rate increases. While η decreases to some value fitting a typical grand unified theory, the curve of energy emission rate declines. This phenomenon presents that a stronger global monopole parameter alter the attribute of emission of a scalar field coupling to the gravitational field. In Fig.8 the influence from $f(R)$ theory on the dependence of the differential energy emission rate on the frequency is described. It is evident that the greater deviation from the standard general relativity leads the curves to drop while moves left. The curves with larger ψ_0 keep more complete feature of emission rate distinctively for low frequency $\omega \ll 1/MG$ and $MG = 1$. The shapes of all of the curves subject to the global monopole parameter and the corrections to the general relativity are similar.

We start to investigate the generalized absorption cross section of a scalar field coupling to the gravitational field in the background of a Schwarzschild black hole with a $f(R)$ global monopole. The absorption cross section for the emission of a particles from a black hole can be defined

as $\sigma \equiv \frac{absorbed\ flux}{incident\ wave\ current}$ leading the expression for asymptotically flat spherically symmetric spacetime as [27],

$$\sigma = \sum_{l=0}^{\infty} \sigma_l = \frac{\pi}{\omega^2} \sum_{l=0}^{\infty} (2l+1)\gamma_l(\omega) \tag{52}$$

where σ_l stands for the absorption cross section of each partial wave. We continue to discuss the condition for applying Eq. (52). We follow Ref. [27] to choose the flux corresponding to the scatted wave and incident current

$$F = \frac{\pi}{\omega} \sum_{l=0}^{\infty} (2l+1)\gamma_l(\omega) \tag{53}$$

$$|\overrightarrow{J}_{inc}| = \omega \frac{r_*^2}{r^2} \sqrt{\frac{1}{f} cos^2\theta + \frac{r_*^2}{r^2} sin^2\theta} \tag{54}$$

Once the incident current equals to ω, Eq. (52) will be confirmed. In matching intermediate region where $M \ll r - r_- \ll 1/\omega$, there exist $f(r) \approx 1 - 8\pi G\eta^2$ and $r_* \approx \frac{r}{1-8\pi G\eta^2}$ for a Schwarzschild spacetime with a f(R) global monopole. If $8\pi G\eta^2 \ll 1$, then $f(r) \approx 1$ and $r_* \approx r$ which yield $|\overrightarrow{J}_{inc}| = \omega$. For this reason, the absorption cross section expression (52) is applicable to the emission in this background only when $8\pi G\eta^2 \ll 1$ and $\psi_0 \sim 0$ for intermediate region. According to the greybody factor (44), we also construct the generalized absorption cross section as a function of frequency in Fig. 9 and Fig. 11. Both the global model parameter η and deviation of general relativity ψ_0 will modify the cross section. It is obvious that almost all curves with different values of η or ψ_0 boil down together while they separate distinctly in low frequency, which conform to the low-energy approximation. From Fig. 9 and the log plot Fig. 10, the larger the cross section in low-frequency becomes as the larger global monopole parameter. Moreover, the curves of the general absorption cross section rise when the variable ψ_0 increases. We notice that while $\omega \to 0$, all the values of $\sigma(0)$ for different ψ_0 and η are finite in Fig. 10 and Fig. 12, and $\omega \to 0$ reduces as ψ_0 and η. It should be pointed out that the shapes of these curves of the generalized absorption cross section associated with the frequency are similar although the cross section is controlled by the global monopole parameter η and variable ψ_0 in the $f(R)$ theory.

VI. Discussion and conclusion

We discuss the greybody factor for massless scalar field in the spacetime of gravitational source involving a global monopole in the context of $f(R)$ gravity theory and we also further study the energy emission rate and generalized absorption cross section. These results all exhibit the effect of global monopole and the influence from $f(R)$ approach. Having matched the two asymptotic solutions to the field equation at the inner and outer horizons respectively, we obtain the acceptable expression of the greybody factor. Further the energy emission rate and the generalized absorption

cross section are also found. It is interesting that the own effects of global monopole model parameter and the variable describing the deviation from general relativity appear in the greybody factor, energy emission rate and the generalized absorption cross section. The greybody factor becomes smaller due to the smaller global monopole parameter with $l = 0$, which is just the contrary with novanishing angular quantum number. The larger the deviation grows, the higher the greybody factor curve rises. Moreover, a distinct feature of the energy emission rate is the curve rises as η reduces when $8\pi G\eta^2 \ll 1$ for the intermediate condition and $8\pi G\eta^2 \approx 10^{-5}$ for a typical unified theory. The emission rate curves fall when η continues decreasing. For $\psi_0 \ll 1$, the greater ψ_0 leads smaller peak values of emission rate in low-energy. The generalized absorption cross section becomes larger with respect to the increasing variable η belonging to the global monopole or increasing ψ_0 to $f(R)$ gravity. As frequency $\omega \to 0$, the values of cross section are finite and drop as η and ψ_0. The cross sections will also be adjusted by the variable ψ_0 as the description of modified general relativity, but their curves keep oscillating around the frequency. The related topics need to be studied in future.

Acknowledge

This work is supported by NSFC No. 10875043 and is partly supported by the Shanghai Research Foundation No. 07dz22020.

References

[1] M. C. Gegelman, Science 300(2003)1898

[2] S. Dimopoulos, G. L. Landsberg, Phys. Rev. Lett. 87(2001)161602

[3] S. B. Giddings, S. D. Thomas, Phys. Rev. D65(2002)056010

[4] J. D. Bekenstein, Lett. Nuovo Cimento 4(1972)737

[5] J. D. Bekenstein, Phys. Rev. D7(1973)2333

[6] J. D. Bekenstein, Phys. Rev. D9(1974)3292

[7] S. W. Hawking, Commun. Math. Phys. 43(1975)199

[8] G. J. Stephens, B. L. Hu, Int. J. Theor. Phys. 40(2001)2183

[9] W. Kim, E. J. Son, M. Yoon, JHEP 0804(2008)042

[10] R. G. Cai, L. M. Cao, N. Ohta, JHEP 1004(2010)082

[11] Y. S. Myung, Y. Kim, Y. Park, Phys. Rev. D78(2008)084002

[12] A. Lala, D. Roychowdhury, Phys. Rev. D86(2012)084027

[13] W. Kim, Y. Kim, Phys. Lett. B718(2012)687

[14] C. Doran, A. Lasenby, S. Dolan, I. Hinder, Phys. Rev. D71(2005)124020

[15] S. Dolan, C. Doran, A. Lasenby, Phys. Rev. D74(2006)064005

[16] L. C. B. Crispino, E. S. Oliveira, A. Higuchi, G. E. A. Matasa, Phys. Rev. D75(2007)104012

[17] S. R. Dolan, Class. Quantum Grav. 25(2008)235002

[18] L. C. B. Crispino, S. R. Dolan, E. S. Oliveira, Phys. Rev. Lett. 102(2009)231103

[19] L. C. B. Crispino, S. R. Dolan, E. S. Oliveira, Phys. Rev. D79(2009)064022

[20] L. C. B. Crispino, A. Higuchi, E. S. Oliveira, Phys. Rev. D80(2009)104026

[21] Y. S. Myung, H. W. Lee, Class. Quantum Grav. 20(2003)3533

[22] T. Harmark, J. Natario, R. Schiappa, Adv. Theor. Math. Phys. 14(2010)727

[23] P. R. Brady, C. M. Chambers, W. Krivan, P. Laguna, Phys. Rev. D55(1997)7538

[24] P. Kanti, J. Grain, A. Barrau, Phys. Rev. D71(2005)104002

[25] M. Liu, B. Yu, R. Wang, L. Xu, Mod. Phys. Lett. A25(2010)2431

[26] S. Wu, S. Yin, G. Yang, P. Zhang, Phys. Rev. D78(2008)084010

[27] L. C. B. Crispino, A. Higuchi, E. S. Oliveira, J. V. Rocha, Phys. Rev. D87(2013)104034

[28] T. W. B. Kibble, J. Phys. A9(1976)1387

[29] A. Vilenkin, Phys. Rep. 121(1985)263

[30] M. Barriola, A. Vilenkin, Phys. Rev. Lett. 63(1989)341

[31] H. A. Buchdahl, Mon. Not. R. Astron. Soc. 150(1970)1

[32] S. Nojiri, S. D. Odintsov. Phys. Rev. D68(2003)125312

[33] S. M. Carroll, V. Duvvuri, M. Trodden, M. S. Turner, Phys. Rev. D70(2004)043528

[34] S. Fay, R. Tavakol, S. Tsujikawa, Phys. Rev. D75(2007)063509

[35] T. R. P. Carames, E. R. B. de Mello, M. E. X. Guimaraes, Int. J. Mod. Phys. A(2011)

[36] T. R. P. Carames, E. R. B. de Mello, M. E. X. Guimaraes, Mod. Phys. Lett. A27(2012)1250177

[37] J. Man, H. Cheng, arXiv: 1205.4857

[38] J. Man, H. Cheng, Phys. Rev. D87(2013)044002

[39] P. Kanti and J. March-Russell, Phys. Rev. D66,024023(2002)
P. Kanti, J. Grain and A. Barran, Phys. Rev. D 71, 104002(2005)

[40] N. D. Birrell, P. C. W. Davies, Quantum Fields in Curved Space, Cambridge University Press, 1982

[41] I. S. Gradshteyn, I. M. Ryzhik, Table of integrals, Series, and Products, Elsevier, New York, 2007

[42] E. Jung, S. Kim and D. Park, JHEP09(2004)005
S. Chen and J. Jing, Phy. Lett. B 691(2010)254

[43] L. Pogosian and A. Silvestri, Phys. Rev. D 77, 023503 (2008)

[44] V. Miranda, S. Joras and I. Waga, Phys. Rev. Lett 102, 221101 (2009)

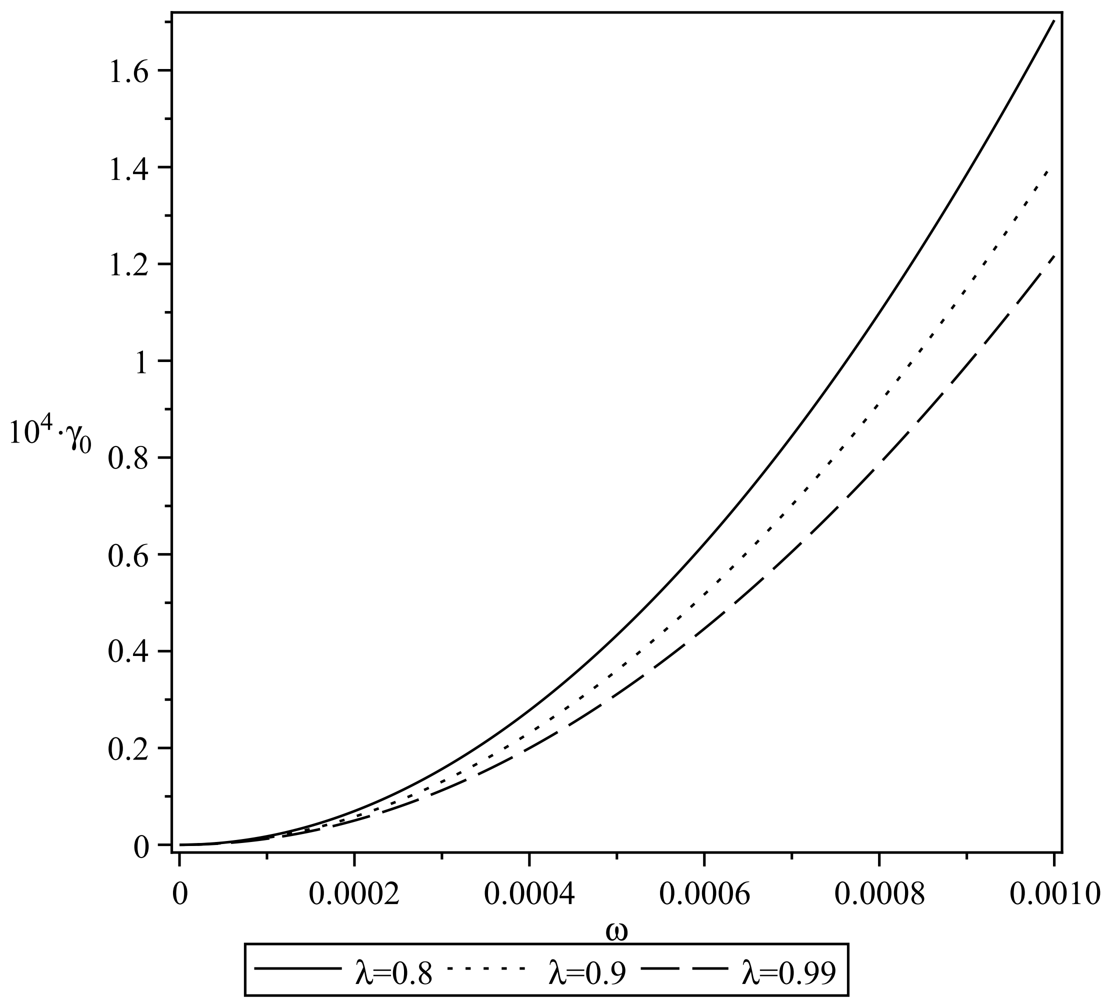

Figure 1: The curves of greybody factor with angular quantum number $l = 0$ as a function of the frequency for $\lambda = 0.8, 0.9, 0.99$ respectively and $\lambda = 1 - 8\pi G\eta^2$, $GM = 10$, $\psi_0 = 0.02$, $\xi = \frac{1}{12}$.

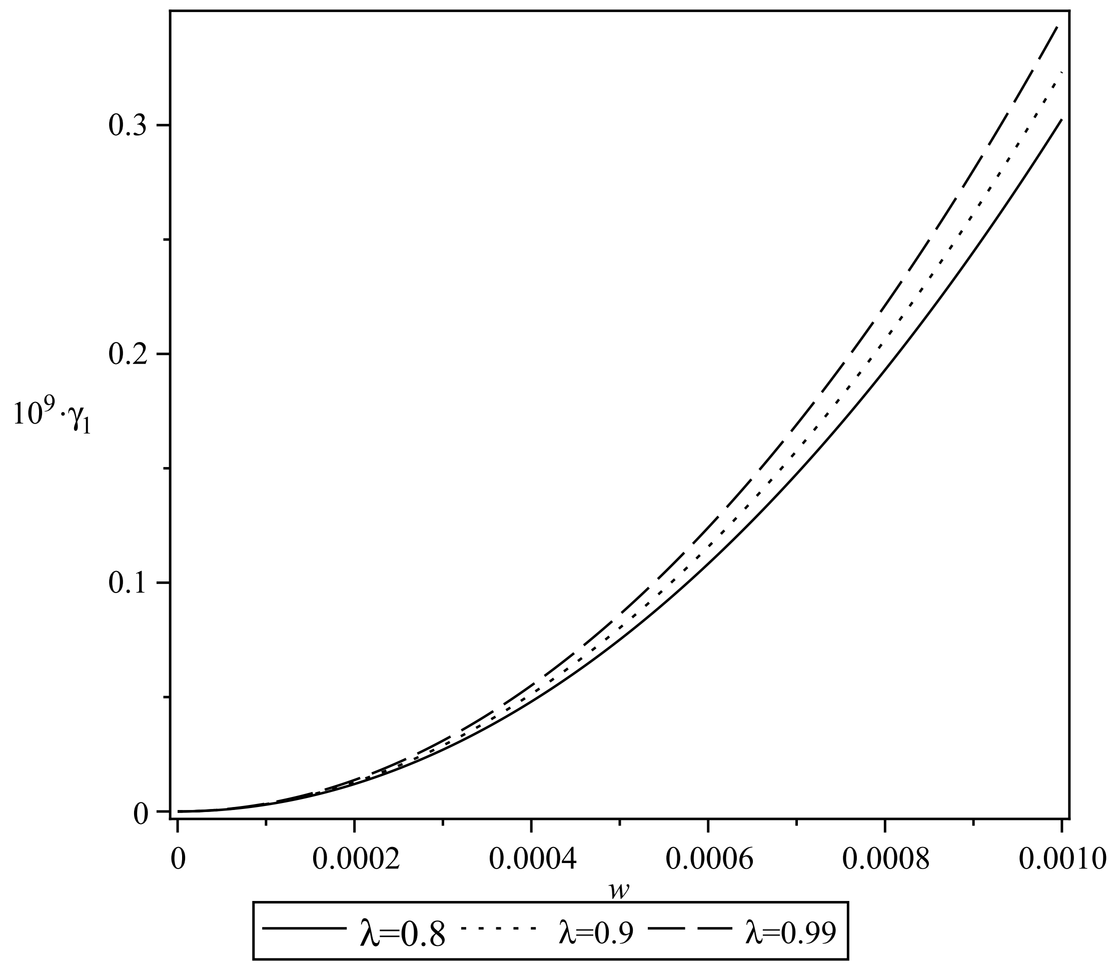

Figure 2: The curves of greybody factor with angular quantum number $l = 1$ as a function of the frequency for $\lambda = 0.8, 0.9, 0.99$ respectively and $\lambda = 1 - 8\pi G\eta^2$, $GM = 10$, $\psi_0 = 0.02$, $\xi = \frac{1}{12}$.

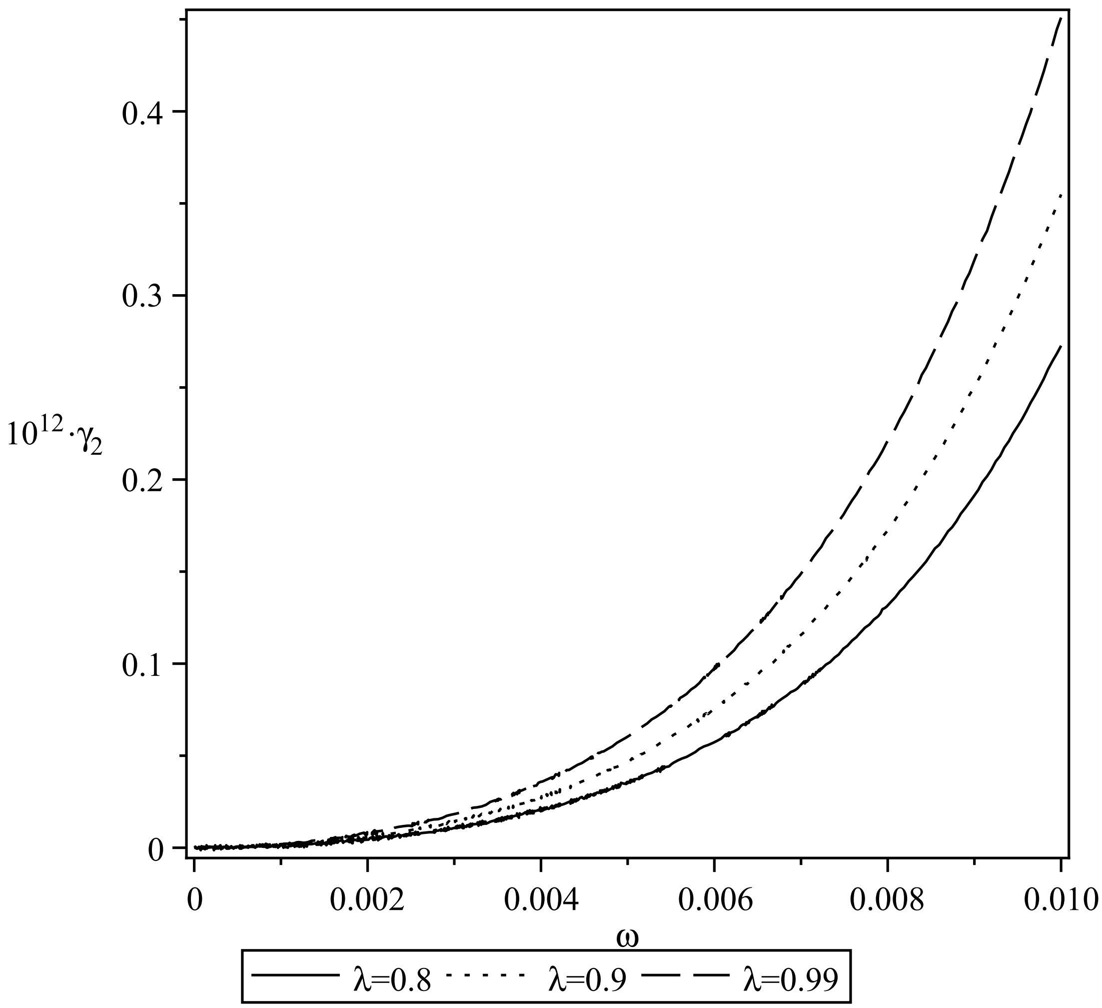

Figure 3: The curves of greybody factor with angular quantum number $l = 2$ as a function of the frequency for $\lambda = 0.8, 0.9, 0.99$ respectively and $\lambda = 1 - 8\pi G\eta^2$, $GM = 10$, $\psi_0 = 0.02$, $\xi = \frac{1}{12}$.

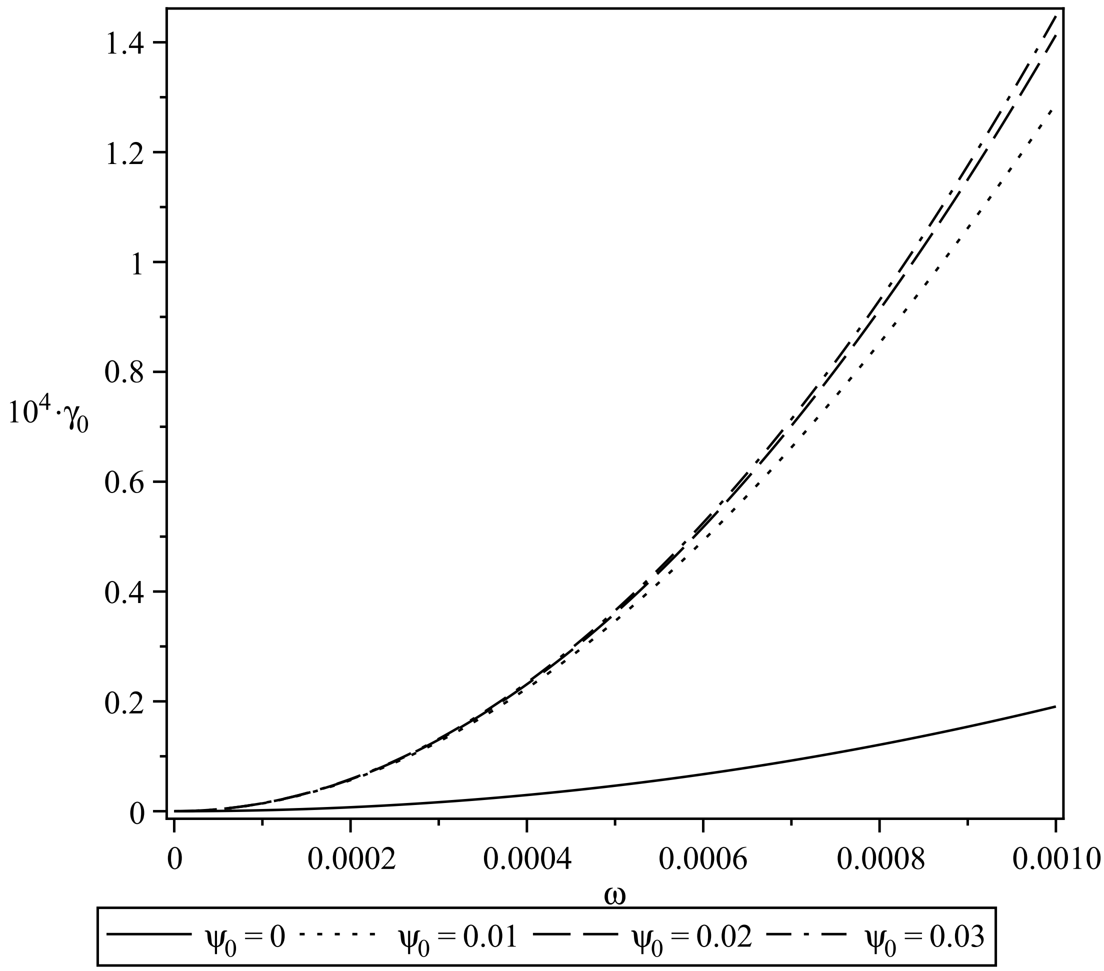

Figure 4: The dependence of Greybody factor for a scalar emission with angular quantum number $l = 0$ on $f(R)$ gravity factor $\psi_0 = 0, 0.01, 0.02, 0.03$ respectively for $GM = 1$, $\lambda = 0.9$, $\xi = \frac{1}{12}$.

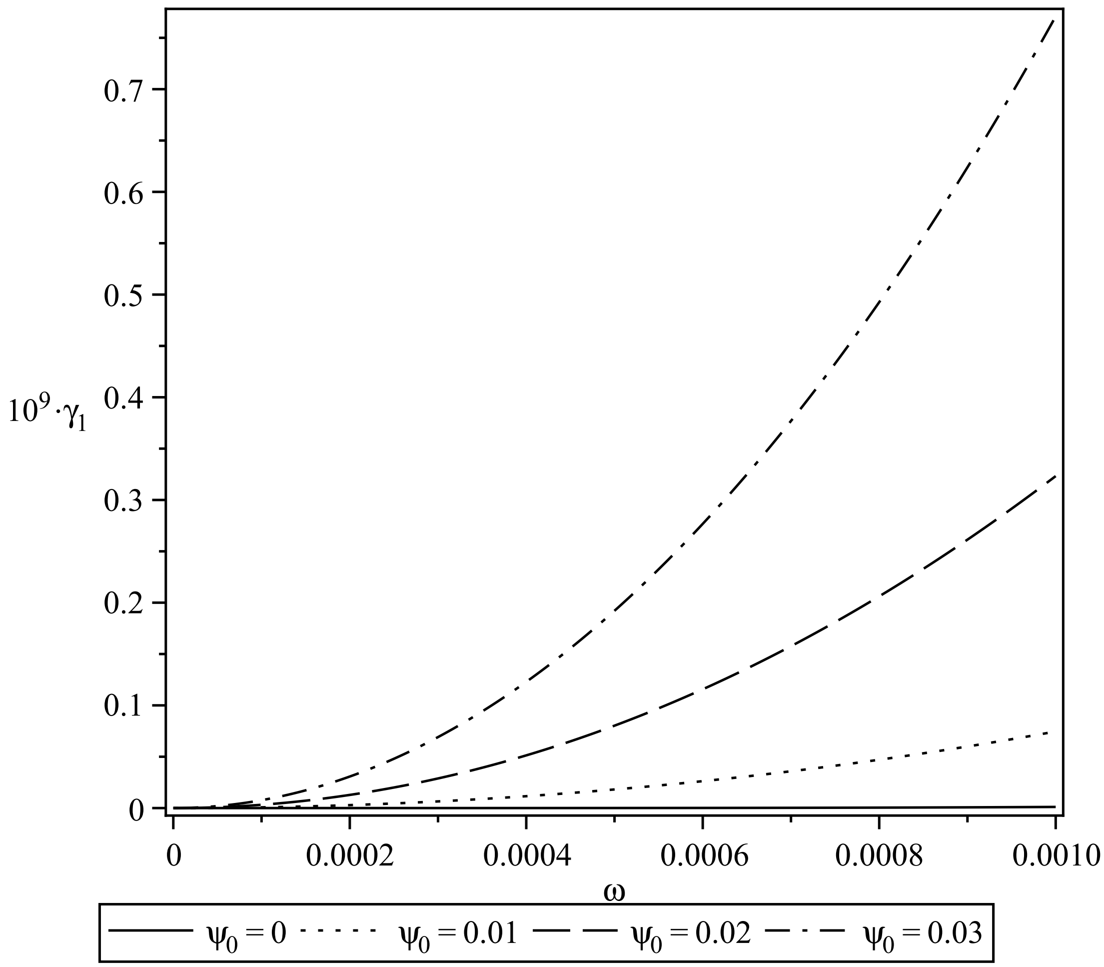

Figure 5: The dependence of Greybody factor for a scalar emission with angular quantum number $l = 1$ on $f(R)$ gravity factor $\psi_0 = 0, 0.01, 0.02, 0.03$ respectively for $GM = 1$, $\lambda = 0.9$, $\xi = \frac{1}{12}$.

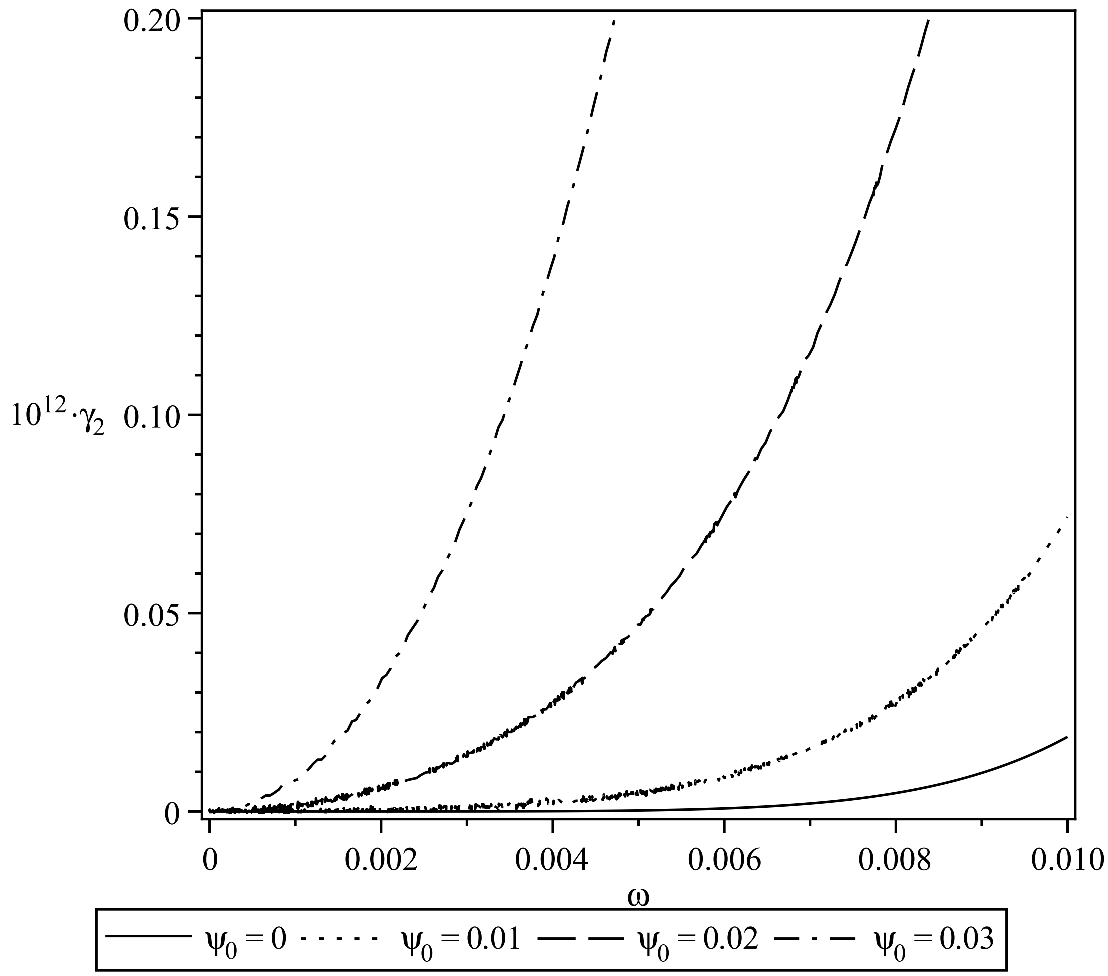

Figure 6: The dependence of Greybody factor for a scalar emission with angular quantum number $l = 2$ on $f(R)$ gravity factor $\psi_0 = 0, 0.01, 0.02, 0.03$ respectively for $GM = 1$, $\lambda = 0.9$, $\xi = \frac{1}{12}$.

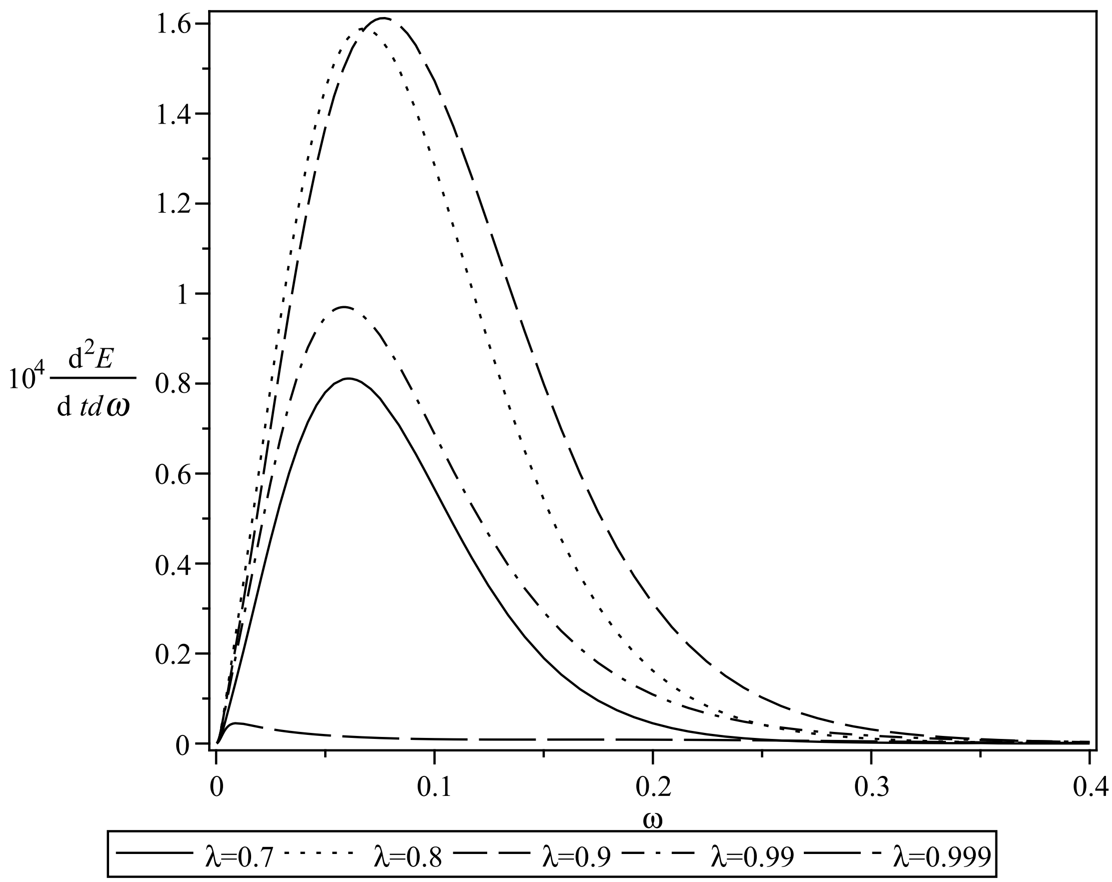

Figure 7: The differential energy emission rate for a scalar emission for various $\lambda = 0.7, 0.8, 0.9, 0.99, 0.999$ and $\lambda = 1 - 8\pi G\eta^2$. Here $GM = 1$, $\psi_0 = 0.02$, $\xi = \frac{1}{12}$

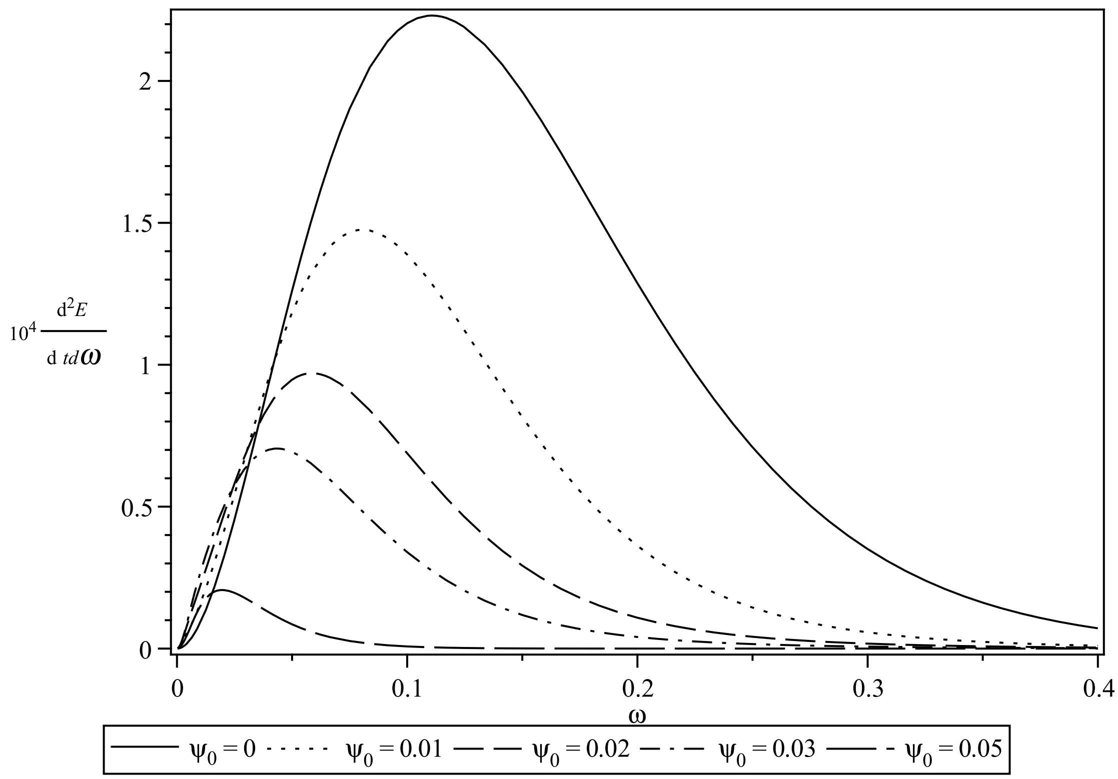

Figure 8: The differential energy emission rate for a scalar emission for different $f(R)$ gravity factor $\psi_0 = 0, 0.01, 0.02, 0.03, 0.05$ respectively. Here $GM = 1$, $\lambda = 0.99$, $\xi = \frac{1}{12}$

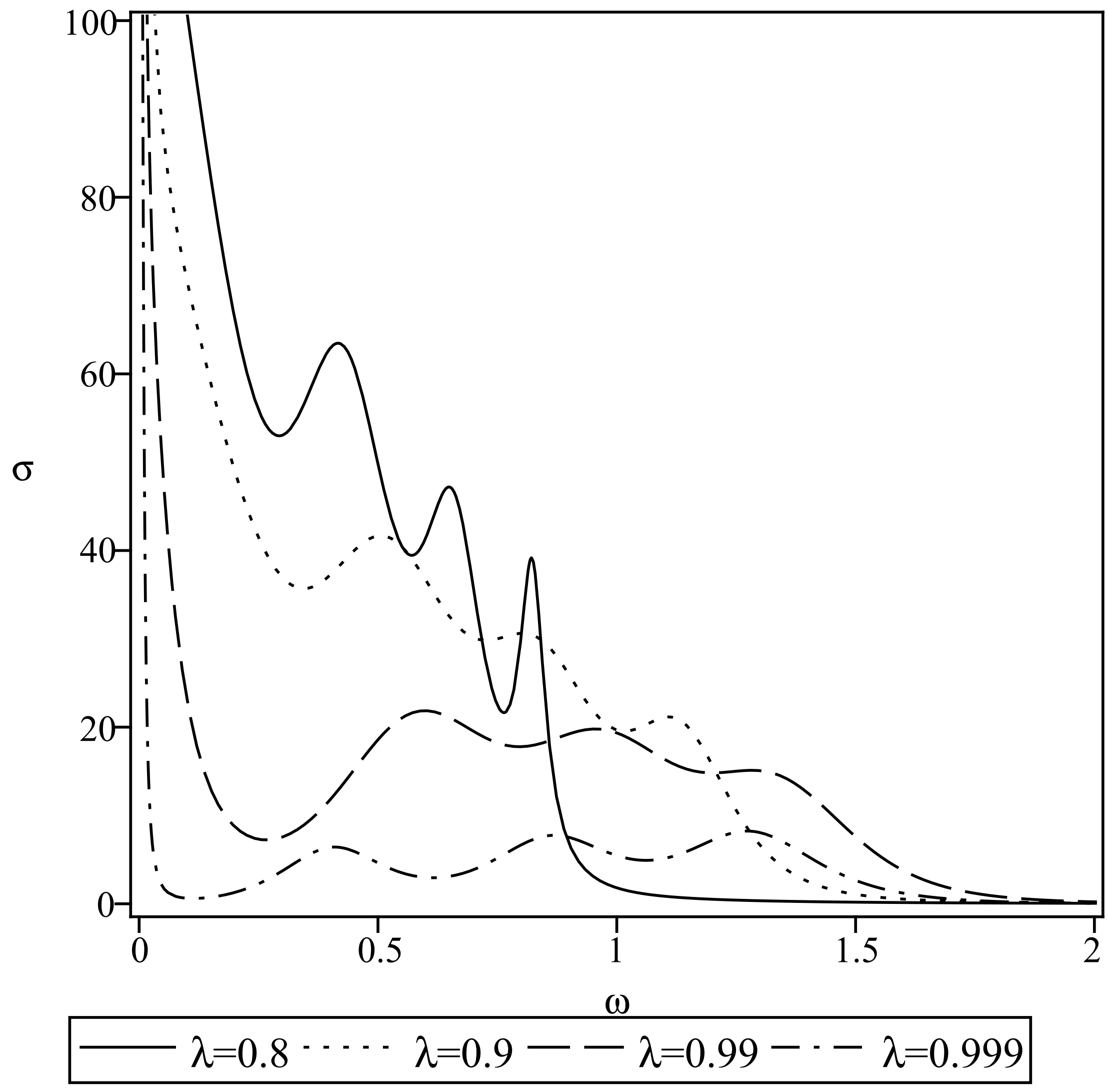

Figure 9: The behavor of the generalized absorption cross section as a function of the frequency for $\lambda = 0.8, 0.9, 0.99, 0.999$ respectively and $\lambda = 1 - 8\pi G\eta^2$. Here $GM = 1$, $\psi_0 = 0.02$, $\xi = \frac{1}{12}$.

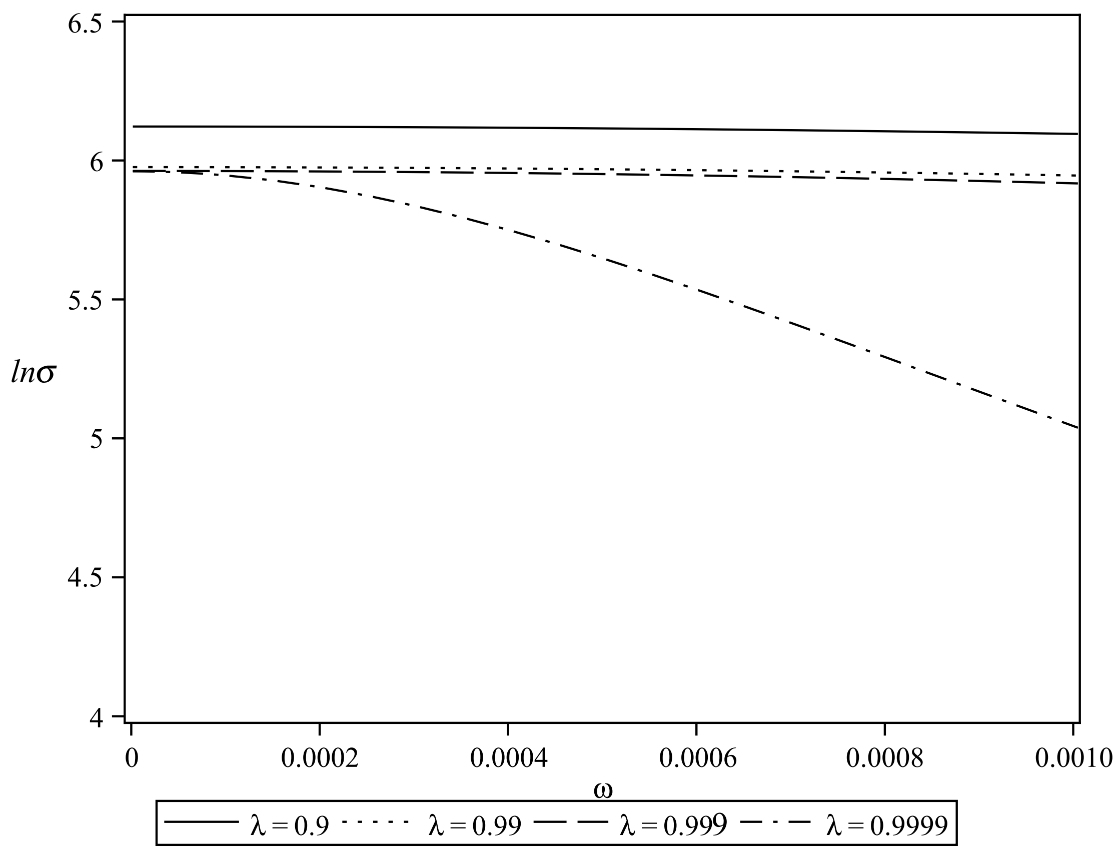

Figure 10: The logarithmic generalized absorption cross section depends on global monopole parameter $\lambda = 0.8, 0.9, 0.99, 0.999$ respectively. Here $GM = 1$, $\psi_0 = 0.02$, $\xi = \frac{1}{12}$.

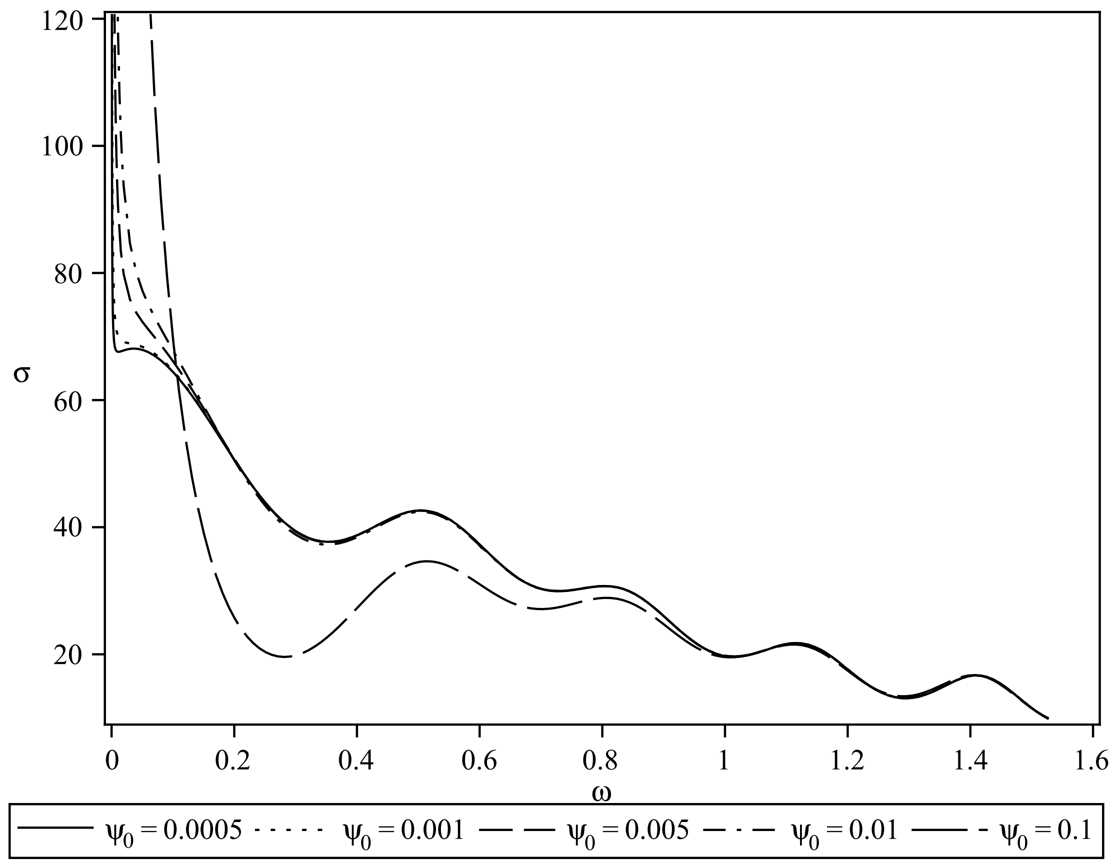

Figure 11: The behavior of the generalized absorption cross section as a function of the frequency for $f(R)$ gravity factor $\psi_0 = 0.0005, 0.001, 0.005, 0.01, 0.1$ respectively. $GM = 1$, $\lambda = 0.9$, $\xi = \frac{1}{12}$.

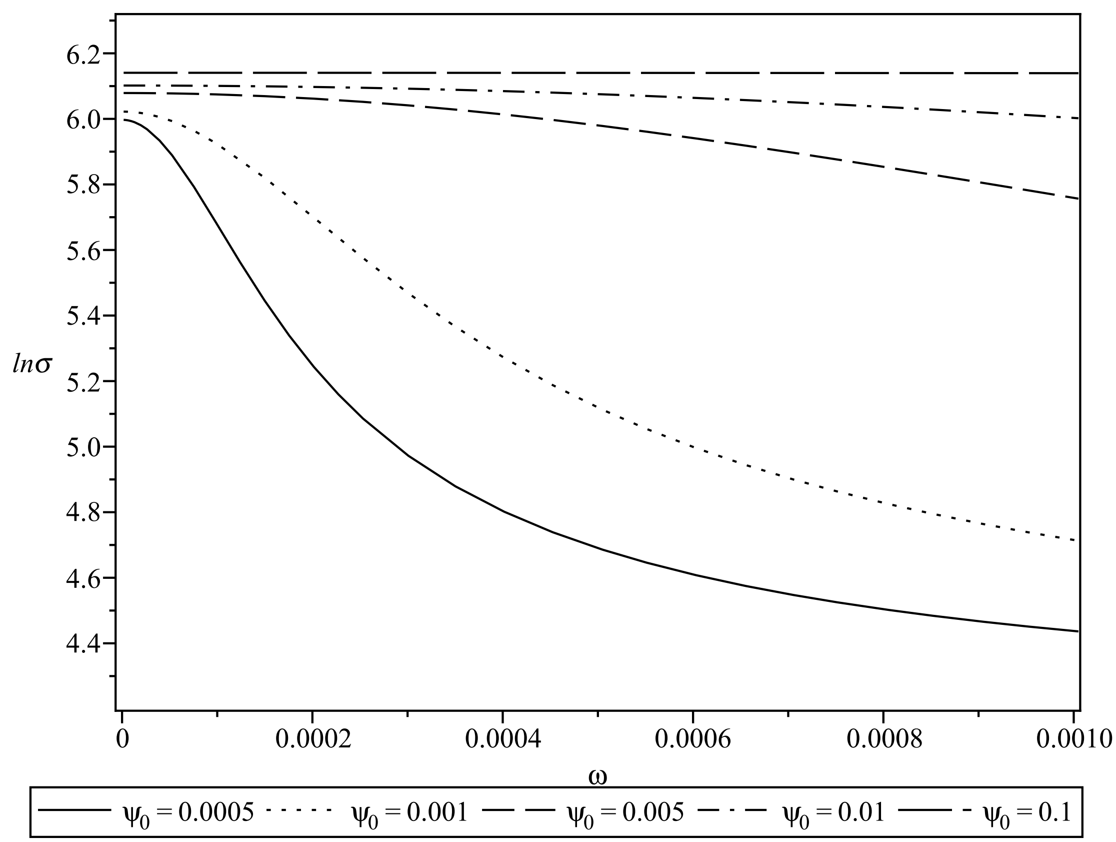

Figure 12: The logarithmic generalized absorption cross section depends on $f(R)$ gravity factor $\psi_0 = 0.0005, 0.001, 0.005, 0.01, 0.1$ respectively.$GM = 1$, $\lambda = 0.9$, $\xi = \frac{1}{12}$.